

## Uncertainty Modeling and Simulation Highlighting on Tail

### Probability in Biomechanics Study on Pressure Ulcer

\*Samuel Susanto Slamet<sup>1</sup>, Naoki Takano<sup>1</sup>, and Tomohisa Nagasao<sup>2</sup>

<sup>1</sup>Keio University, Faculty of Science and Technology, Department of Mechanical Engineering  
3-14-1 Hiyoshi, Kohoku-ku, Yokohama, Kanagawa, Japan

<sup>2</sup>Keio University, School of Medicine, Department of Plastic Surgery  
35 Shinanomachi, Shinjuku-ku, Tokyo, Japan

\*Corresponding author: samuel@z7.keio.jp

#### Abstract

This paper aims at building up a computational procedure to study the bio-mechanism of pressure ulcer using the finite element method. Pressure ulcer is a disease that occurs in the human body after 2 hours of continuous external force. This study assumes that tension and/or shear strain will cause damage to loose fibril tissue between the bone and muscle and that propagation of damaged area will lead to fatal stage. Analysis was performed using the finite element method by modeling the damaged fibril tissue as a cutout. Various uncertainties such as the material properties, loading condition, location of cutout, the length of cutout and configuration of the human buttock were considered in this analysis. By watching both tensile and shear strains, the risk of fibril tissue damage and propagation of the damaged area is discussed and the results may give new insights for careful nursing of patients.

**Keywords:** FEM, Pressure ulcer, Interface strain, Tail probability, Monte Carlo simulation

#### Introduction

The pressure ulcer occurs by sustained pressure and cutoff of blood supply. It has been found that internal damage in deep muscle layers covering bony prominences result in fatal pressure ulcer (Bouten et al., 2003; Maeda, 2006). However, the initial location of that damage is unknown. The final goal of the developed biomechanics simulation is to obtain the set of dangerous material parameters for muscle and fat that can lead to high strain at the bone-muscle interface depending on the load condition under different body positions

The Markov Chain Monte Carlo methods are well known methods to consider any kind of uncertainty (Shenk and Shueller, 2005; Gamerman and Lopez, 2006; Rubinstein and Kroese, 2009). Its demerit is the computational cost required to obtain reliable probability density of the quantity of interest (QoI). Also, the accuracy of Monte Carlo simulation depends on the generation of random numbers algorithm and the number of computational cases.

In this study a practical sampling algorithm named Stepwise Limited Sampling (SLS) is proposed to obtain both accurate enough expected value and the tail probability accurately in the Monte Carlo simulation. It is then applied to a biomechanics problem on the risk prediction of the pressure ulcer.

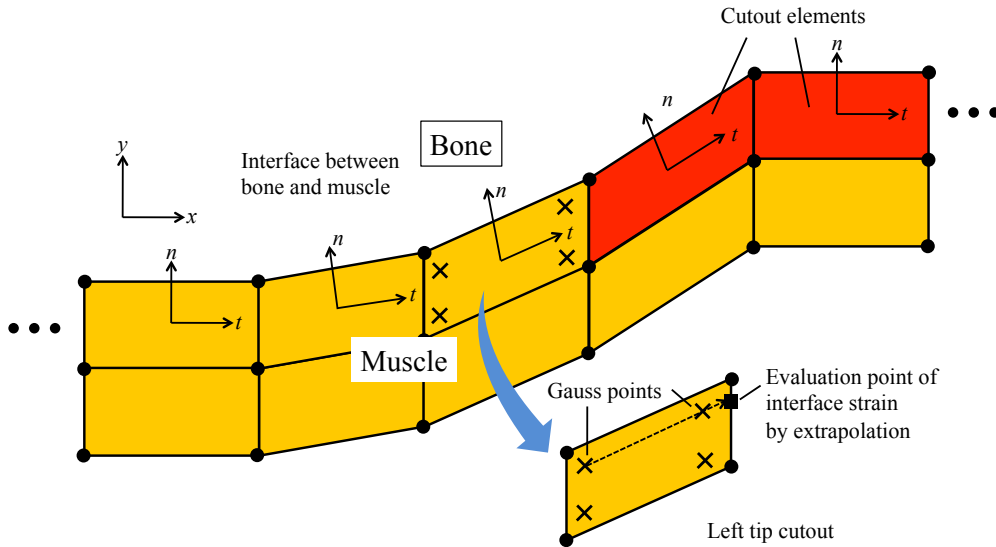


**Figure 1. Quantity of interest (QoI)**

The authors have so far proposed a simplified numerical modeling by assuming that the initial damage occurs at the interface between bone and muscle by the loose fibril tissue damage, in which the risk of reoccurrence of pressure ulcer after surgery was successfully evaluated (Slamet et al. 2012). Also we pointed out that severe shear loading to the patient's buttock might become a trigger of pressure ulcer. The same bio-mechanism assumption is employed in this paper and the interface damage is modeled by a cutout in finite element model.

In the biomechanics analysis of pressure ulcer where the fibril tissue damage at the interface between bone and muscle is modeled by cutout, the strains at the left and right cutout tips are the quantity of interest. The strains are transformed into normal ( $n$ ) and tangential ( $t$ ) coordinate system along the interface as shown in Fig. 1. The cutout tip strain is extrapolated from the values at Gauss points in the neighboring element, so that the extrapolation can be automated. We denote normal strain and shear strain  $\varepsilon_n$  and  $\gamma_{tn}$ . Concerning normal strain  $\varepsilon_n$ , it is assumed that only tensile strain contributes to the breakage of fibril tissue and propagation of damage area.

### **Mathematical Parameters and Numerical Models of Pressure Ulcer**

In this paper, 2D linear finite element analysis is carried out in the same way with the authors' previous paper (Slamet et al. 2012). Figure 2 shows a typical image of healthy human buttock. Bone, muscle, fat and skin are the main tissues, and the center part is the target region where muscle covering bony prominences is seen. The skin was neglected because Makhous et al. reported that the deformation of skin was much smaller than that of muscle and fat. So only the Young's modulus, Poisson's ratio and Shear modulus of bone, fat and muscle are considered in this analysis represented by  $E_{fat}$ ,  $E_{muscle}$ , and  $E_{bone}$  for the Young's modulus of fat, muscle and bone,  $\nu_{fat}$ ,  $\nu_{muscle}$  and  $\nu_{bone}$  for Poisson's ratio of fat, muscle and bone and  $G_{fat}$ ,  $G_{muscle}$  and  $G_{bone}$  for the shear modulus of fat, muscle and bone.

The curve of the model is defined as  $I_{out}$ ,  $I_{fm}$ , and  $I_{mb}$  where each represents outline form, curve between fat and muscle, and curve between muscle and bone.

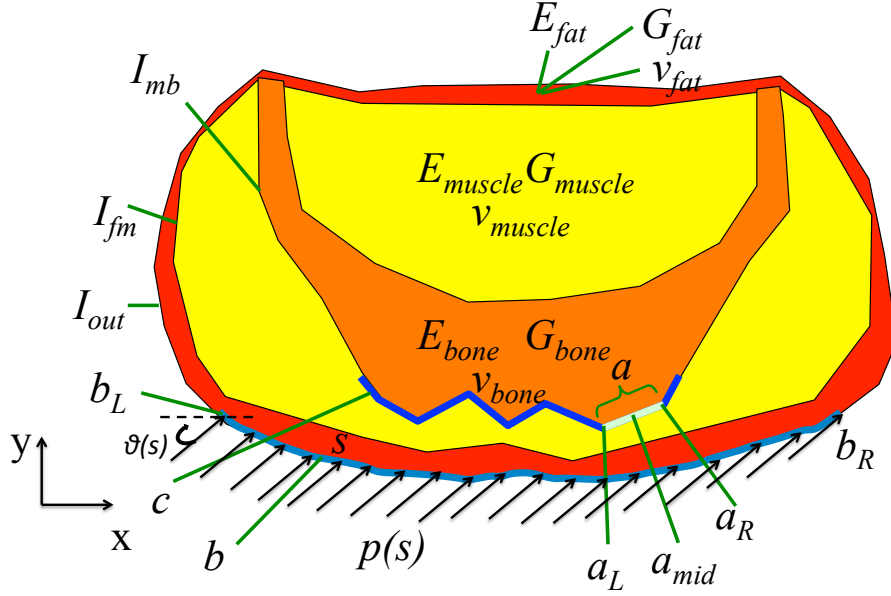


**Figure 2. Mathematical model parameters**

The fibril tissue damage was modeled by a cutout. The location of possible cutout is located in  $c$ , which is an element of  $I_{mb}$ . The location of cutout is then defined as  $a$  as an element of  $c$  with the center location as  $a_{mid}$ , length of cutout as  $L_a$  and left and right edges as  $a_L$  and  $a_R$ .

Contact area or loading area for the model is defined as  $b$ , which is an element of  $I_{out}$ . The left edge and right edge of the loading area is defined as  $b_L$  and  $b_R$ . The loading value itself is defined as  $p(s)$  with  $s$  as the curve along  $b$ . There is also a loading angle of  $\theta$ .

**Table 1. Phenomena identification and ranking table**

Description		Parameter Involved	Importance	
Inter-individual difference	Age	-	High	
	Gender	-	High	
	Geometry	Contour	$I_{out}$	High
		Configuration of fat and muscle	$I_{fm}$	High
		Configuration of bone	$I_{mb}$	High
	Material properties	Skin	-	Low
		Fat	$E_{fat}, G_{fat}$	High
		Muscle	$E_{muscle}$	High
		Bone	-	Low
	Loading area	Area	$b$	High
		Direction	$\theta(s)$	High
Load value		$p(s)$	High	
Cutout	Location	$a_{mid}$	High	
	Length	$L_a$	High	

**Table 2. Material properties**

	Young's modulus, E (MPa)		Shear modulus, G (MPa)		Coefficient of correlation between E and G	Poisson's ratio, $\nu$
	Mean value	Standard deviation (normal distribution)	Mean value	Standard deviation (normal distribution)		
Fat	$8.0 \times 10^{-2}$	$8.0 \times 10^{-3}$	$2.857 \times 10^{-2}$	$2.857 \times 10^{-3}$	0.995	0.4
Muscle	$7.5 \times 10^{-2}$	$7.5 \times 10^{-3}$	$2.517 \times 10^{-2}$	-	-	0.49
Bone	$2.0 \times 10^4$	-	-	-	-	0.3

Uncertainties were considered in 7 areas as seen in Table 1. Location of cutout ( $a_{mid}$ ) with 3 different sampling locations, length of cutout ( $L_a$ ) with 2 different sampling lengths, loading condition ( $b$ ) with 3 different loading sampling and configuration of muscle and fat ( $I_{fm}$ ) with 2 different sampling configurations, and 3 random input parameters in Young's modulus of fat ( $E_{fat}$ ), shear modulus of fat ( $G_{fat}$ ) and Young's modulus of muscle ( $E_{muscle}$ ).

Table 2 shows the material properties based on linear isotropic model. A normal distribution is assumed for simplicity. The coefficient of correlation between Young's modulus and shear modulus for fat was determined so that the Poisson's ratio does not exceed 0.5. For muscle, only the variation of Young's modulus was considered because its Poisson's ratio is close to 0.5. For cutout element,  $10^{-5}$  times smaller value than the mean Young's modulus of muscle was used.

The numerical values for geometry, loading area and cutout can be seen in table 3.

### Stepwise Limited Sampling (SLS) Method

By giving the random distribution with relatively large scattering, the Monte Carlo method provides us the probability density of the quantity of interest, its expected value and standard deviation. It is known that analyses of 10,000 cases are usually required to reach the convergence of both expected value and standard deviation. The accuracy is dependent on the generation scheme of random numbers. The Mersenne Twister is known to give high quality random numbers and it is used in this study too.

The convergence of the expected value is, in general, more easily obtained than standard deviation. One of the reasons is that the quality of random numbers generated in the tail probability is not good enough among 10,000 random numbers even if Mersenne Twister method is adopted. In other words, if one wants to put highlight on the reliability of the tail probability, 10,000 cases are not enough. It is important, for instance, when the prediction of fracture/failure is required even if its probability is very low. Considering that the demerit of Monte Carlo simulation is the high computational cost, a new and cost-effective sampling scheme highlighting on the tail probability would be valuable in vast industries.

Therefore, a Stepwise Limited Sampling (SLS) is proposed in this paper, which stops the iteration when the expected value is converged and spends the computational time for the analyses of the cases in tail probability.

**Table 3. Numerical values for geometry, loading area and cutout.**

Description		Sampling points	Values		
Geometry	$I_{fm}$	$I_{fm1}$	Muscle-rich		
		$I_{fm2}$	Fat-rich		
Loading area	$b$	$b_1$	Supine	$b_L$	(39, 109) mm
				$b_R$	(447, 108) mm
				$p(s)$	$0.8 \times 10^{-2}$ MPa
				$\theta(s)$	$90^\circ$
		$b_2$	Lateral-A	$b_L$	(38, 290) mm
				$b_R$	(28, 120) mm
				$p(s)$	$1.8 \times 10^{-2}$ MPa
				$\theta(s)$	$0^\circ$
		$b_3$	Lateral-B	$b_L$	(470, 133) mm
				$b_R$	(438, 290) mm
				$p(s)$	$1.8 \times 10^{-2}$ MPa
				$\theta(s)$	$180^\circ$
Cutout	$a_{mid}$	$a_{mid-1}$	Left	(186, 100) mm	
		$a_{mid-2}$	Center	(229, 91.9) mm	
		$a_{mid-3}$	Right	(283, 90.5) mm	
	$L_a$	$L_{a-1}$	Left	$L_a$	4 mm
				$a_L$	(184.30, 98.86) mm
				$a_R$	(187.65, 101.10) mm
			Center	$L_a$	4 mm
				$a_L$	(227.70, 92.86) mm
				$a_R$	(230.57, 90.95) mm
		Right	$L_a$	4 mm	
			$a_L$	(281.70, 91.50) mm	
			$a_R$	(285.26, 89.52) mm	
			$L_{a-2}$	Left	$L_a$
		$a_L$			(182.62, 97.74) mm
		$a_R$			(189.33, 102.22) mm
		Center		$L_a$	8 mm
				$a_L$	(226.30, 93.80) mm
				$a_R$	(231.97, 90.02) mm
		Right		$L_a$	8 mm
			$a_L$	(279.96, 92.46) mm	
$a_R$	(287, 88.55) mm				

SLS only assures the moderate accuracy of expected value of quantity of interest. The expected value itself is distributed and therefore the convergence is estimated based on the central limited theorem. Let  $E_{(i)}$  be the expected value and  $\sigma_{(i)}$  be the standard deviation after  $i$  sets of analyses in standard Monte Carlo simulation. The convergence is judged by Eq. (1)

$$E_{(i)} - E_{(i-1)} \leq \frac{\sigma_{(1)}}{E_{(1)}\sqrt{n_{\max}}} \quad (1)$$

where right hand side is normalized by the expected value after the first set of analyses. We recommend to use  $n_{max} = 10,000$ . Let 100 cases be one set of analyses, then Eq. (1) yields as follows.

$$E_{(100j)} - E_{(100(j-1))} \leq \frac{\sigma_{(100)}}{E_{(100)} \sqrt{n_{max}}} \quad (2)$$

If Eq. (2) holds three times continuously, then the expected value is converged. This is because the expected value may oscillate in the Monte Carlo simulation. When the convergence is obtained, the Monte Carlo simulation is suspended.

Next, as the post-processing, the correlation between the input parameters sets and the quantity of interest must be investigated. Supposing that the number of parameters is large, sets of two parameters among all parameters are chosen. Then the quantity of interest can be plotted in the two-dimensional space of the parameters. To this end, it is easy to determine the limited zone with specific value of quantity of interest by the following equation.

$$p_i x_i + p_j x_j + q \geq 0 \quad (i \neq j) \quad (3)$$

Here,  $x_i$  and  $x_j$  are the chosen two parameters, and  $p_i$ ,  $p_j$  and  $q$  are scalar factors. By the combination of multiple linear equations, Eq. (3), in the multi-dimensional space of all parameters, the limited zone to be analyzed carefully can be defined. This procedure is automated in the program, because simple linear equations are used.

### Analysis and Discussion

There are a total of 36 models considering by consideration of 4 uncertainties of configuration of fat and muscle, loading area, location of cutout and length of cutout, with each model having 3 random input parameters of  $E_{fat}$ ,  $G_{fat}$  and  $E_{muscle}$ . All uncertainty parameters are modeled using the finite element mesh as shown in Fig. 3. A total of 77,334 four-noded elements were used in the analysis.

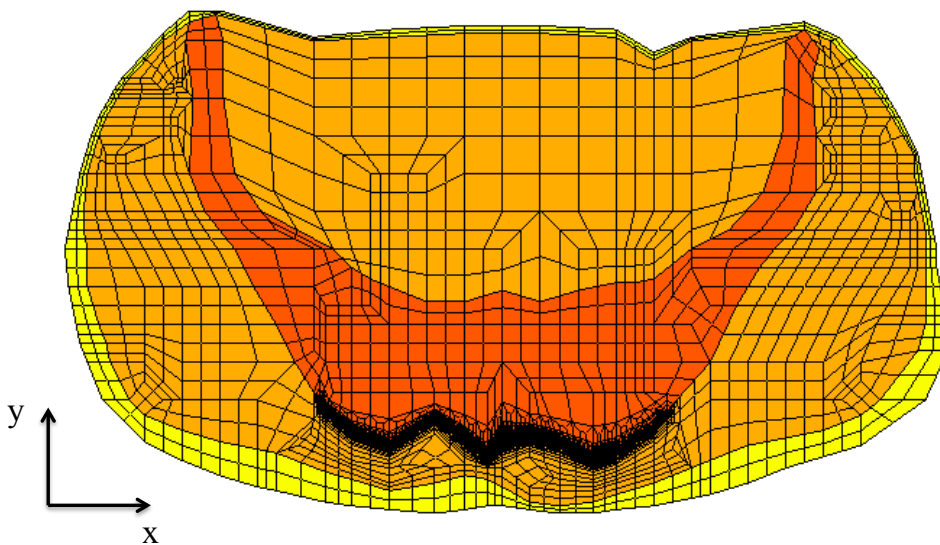


**Figure 3. A typical mesh used for 36 data analyses.**

Each model then had a convergence check to decide when the analysis should be stop. The convergence of the models varies between 1,300 analyses to 4,900 analyses. The limited area is then decided for each model from the three-dimensional space of random parameters  $E_{fat}$ ,  $G_{fat}$  and  $E_{muscle}$ .  $\mu + 3\sigma$  was used as the threshold of limited dangerous zone.

The limited zone was originally defined by combinations of  $E_{fat} - G_{fat}$  and  $E_{fat} - E_{muscle}$ , but the results of  $E_{fat} - G_{fat}$  shows the same formula as  $E_{fat} - E_{muscle}$ , so only  $E_{fat} - E_{muscle}$  are then plotted into the limited sampling zone.

After the process of convergence check and deciding the limited area for all 36 models, the results from those six-dimensional space are then put into a two-dimensional space as seen in Fig. 4. The six-dimension space starts from  $L_a$  and in Fig. 4 case is  $L_a = 4$  mm. From there, 2 main axes were considered, one axis is for  $I_{fm}$  and another one is for  $a_{mid}$ . In the  $I_{fm}$  axis, the  $a_{mid}$  (shown in dotted line for  $a_{mid-1}$ , solid line for  $a_{mid-2}$  and dashed line for  $a_{mid-3}$ ) and  $b$  (shown in blue for  $b_1$ , red for  $b_2$  and green for  $b_3$ ) are compacted into 2 figures with one figure for  $I_{fm-1}$  and another for  $I_{fm-2}$ . In the  $a_{mid}$  axis, the  $I_{fm}$  (shown in solid line for  $I_{fm-1}$  and dotted line for  $I_{fm-2}$ ) and  $b$  (shown in blue for  $b_1$ , red for  $b_2$  and green for  $b_3$ ) are compacted into 3 figures with one figure for  $a_{mid-1}$ , another for  $a_{mid-2}$  and  $a_{mid-3}$ . The figures on the axes of  $I_{fm}$  and  $a_{mid}$  itself contain a two-dimensional projection of the limited zone for  $E_{fat} - E_{muscle}$ . Linear interpolation was applied for simplicity to predict the limited zone between  $a_{mid-2}$  and  $a_{mid-3}$ .

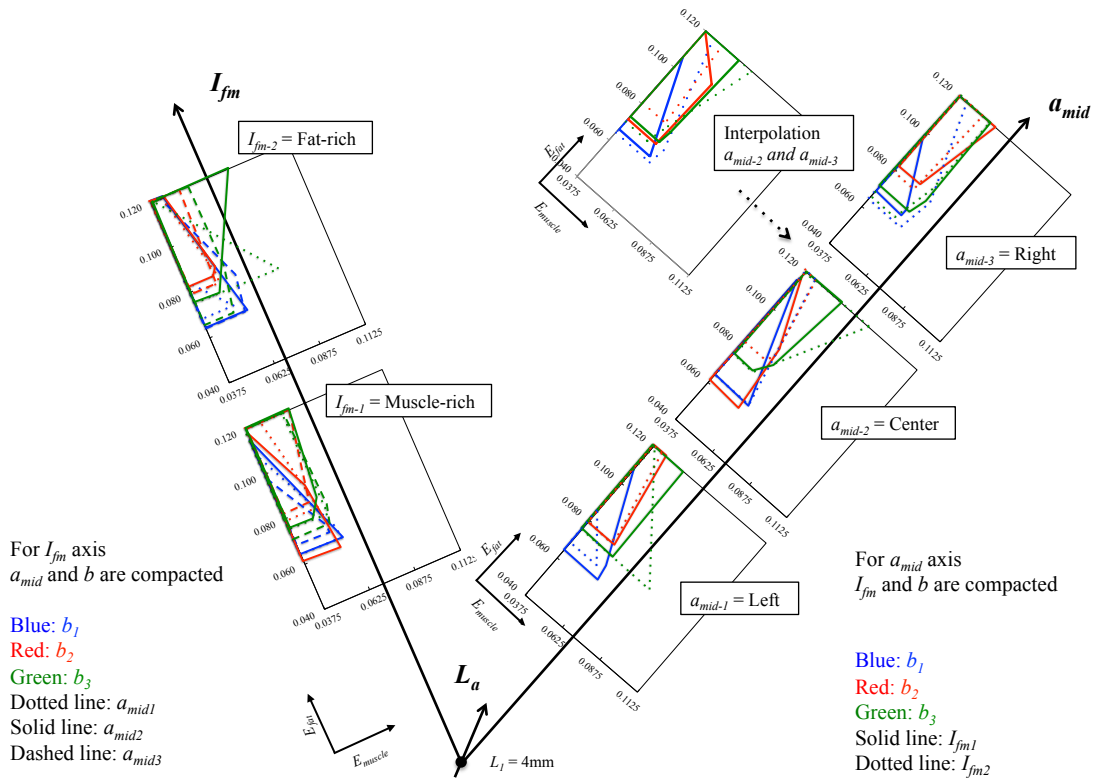


Figure 4. Six-dimensional space of the limited sampling zone on  $L_a = 4$  mm

After determining the limited zone in this way, medical doctors can then predict set of limitation that can lead to pressure ulcers by looking into the corresponding parameters. This will prove useful for nursing patients to prevent the occurrence of pressure ulcer.

## Conclusions

In order to reduce the computational cost of Monte Carlo analysis, a sampling algorithm method was proposed. Seven uncertainty parameters were put into consideration in this analysis with the goal to find a new finding from the clinical viewpoint by predicting the dangerous zone of pressure ulcer. The correlation between geometry, loading area, cutout location, cutout length, and random material parameters at the interface between the bone and muscle was calculated. Medical doctors can find set of parameters that leads to high interface strain in order to prevent the occurrence of pressure ulcer from happening.

The computational time was completely reduced in this analysis compared to the conventional Monte Carlo simulation. The method shown here is cost-effective and practical.

In future works, the biomechanics simulation should contain more random parameters such as age and gender as mentioned in the phenomena identification and ranking table due to its high importance. The SLS algorithm is applicable to a problem with larger input parameters as shown in this paper, and it should be proven to be able to handle more parameter in future simulation. The applied interpolation should also be validated which can lead to finding the response surface along all possible cutout locations and different fat and muscle configurations.

Although 2D linear analyses were carried out as a demonstration in this paper, 3D non-linear analyses should be employed in the future, considering large deformation, contact between body and bed and viscoelasticity.

## References

- Bouten, C. V., Oomens, C. W., Baaijens, F. P. and Bader, D. L., *The Etiology of Pressure Ulcers: Skin Deep or Muscle Bound*, Archives of Physical Medicine and Rehabilitation, 84, 2003, pp. 616-619.
- Maeda, T., *Pressure Ulcers Resulting from Earlier and More Marked Injury in the Deeper Layers - Typical Clinical Cases and an Insight into Pocket Formation*, Japanese Journal of Pressure Ulcers, 8, 2006, pp. 195-202 (in Japanese).
- Shenk, C. A. and Shueller, G. I., *Uncertainty Assessment of Large Finite Element Systems*, Springer, Berlin, 2005.
- Gamerman, D. and Lopez, H. F., *Markov Chain Monte Carlo*, Chapman & Hall, London, 2006.
- Rubinstein, R. Y. and Kroese D. P., *Simulation and the Monte Carlo Method*, John Wiley & Sons, New Jersey, 2009.
- Slamet, S. S., Takano, N., Tanabe, Y., Hatano, A. and Nagasao, T., *Biomechanics Analysis of Pressure Ulcer using Damaged Interface Model between Bone and Muscle in the Human Buttock*, Journal of Computational Science and Technology, 6, 2012, pp. 70-80.
- Makhsous, M., Lim, D., Hendrix, R., Bankard, J., Rymer, W. Z. and Lin, F., *Finite Element Analysis for Evaluation of Pressure Ulcer on the Buttock: Development and Validation*, IEEE Transactions on Neural Systems and Rehabilitation Engineering, 15, 2007, pp. 517-525.